

# High-Tensile-Property Layered Silicates/Polyurethane Nanocomposites by Using Reactive Silicates as Pseudo Chain Extenders

Y. I. Tien and K. H. Wei\*

Department of Materials Science and Engineering, National Chiao Tung University, Hsinchu, Taiwan 30049, R.O.C.

Received April 2, 2001; Revised Manuscript Received October 8, 2001

**ABSTRACT:** Tethered layered silicates/polyurethane nanocomposites displaying high tensile strength and high elongation to break were synthesized by using reactive swelling-agent-modified silicates as pseudo chain extenders for a polyurethane prepolymer. The dispersion of layered silicates in polyurethane was found to be transformed from an intercalated to an exfoliated structure when the number of hydroxyl groups of the swelling agent increased as evidenced from the transmission electron microscopy and wide-angle X-ray diffraction analyses. The improved morphology of the nanocomposites resulted in an ultrahigh efficiency in enhancing the mechanical properties of polyurethane, despite variations in the molecular weight and in the extent of hydrogen bonding in the hard segment phase. In particular, a 34% increase in Young's modulus, a 1.7-fold increase in the tensile strength, and a 1.3-fold increase in the elongation to break occurred in the nanocomposite of polyurethane containing only 1 wt % trihydroxyl-group swelling-agent-modified silicates as compared to those of pristine polyurethane.

## Introduction

Polyurethane is a segmented polymer that is well-known for its biocompatible, elastic, and abrasive properties. The two-phase morphology of polyurethane is a result of the incompatibility between the soft and hard segments. The morphology of polyurethane determines its mechanical, thermal, and water absorption properties.<sup>1–3</sup> The hard-segment phase is made up of hydrogen-bonded stiff segments that were formed by a reaction of diisocyanate with chain extender. The extent of hard segments primarily determines the modulus of polyurethane, but this phase also degrades easily at temperatures above 200 °C. The flexible soft-segment phase, which is composed of polyether or polyester diol, predominately influences the elastic nature of polyurethane.

Nanocomposites are usually defined as composites having more than one solid phase with a dimension of less than 100 nm.<sup>4–7</sup> Layered silicates/polymer nanocomposites have recently attracted a great deal of attention because of the improvements in the mechanical, thermal, and gas barrier properties of the polymer. These improvements are brought about by having a small amount of layered silicates dispersed at the nanometer scale. Polymer nanocomposites such as polyamide,<sup>8–10</sup> epoxy,<sup>11,12</sup> polystyrene,<sup>13,14</sup> poly(ethylene oxide),<sup>15,16</sup> polycaprolactone,<sup>17</sup> polyimide,<sup>18–22</sup> and polyurethane<sup>23–29</sup> with montmorillonite or layered silicates have been developed. Montmorillonite consists of layered silicates belonging to the 2:1 phyllosilicate, and the crystal structure of silicate layers is made of two silica tetrahedrally fused to an edge-shared octahedral sheet of either aluminum or magnesium hydroxide. Natural montmorillonite is composed of 1-nm-thick layered silicates whose diameter lies typically between 20 and 1000 nm. A 100-nm diameter and a 1-nm thickness are used to represent the average dimensions of the disklike cross section in this work. These silicates self-organize

to form stacks with a regular van der Waals gap between the intergalleries. Isomorphic substitution within the layers (e.g., Al<sup>3+</sup> replaced by Mg<sup>2+</sup> or Fe<sup>2+</sup>) generates negative charges that are counterbalanced by cations (Na<sup>+</sup>, Ca<sup>2+</sup>, or K<sup>+</sup>) residing in the gallery space.<sup>30</sup> The existence of these ionic bonds and the ability to form hydrogen bonds with water make montmorillonite highly hydrophilic and incompatible with organic polymers. To disperse the silicates in the polymer, it is necessary to modify the montmorillonite with various organic cationic molecules (which are defined as swelling agents here) to render the silicates organophilic.

In previous synthetic routes to silicate/polyurethane nanocomposites, the approach was to physically mix alkyl- or aromatic-modified silicates with polyurethane prepolymer or polyurethane urea polymer in solvents.<sup>23–25,27,28</sup> The production of intercalated silicates resulted from physical trap forces such as polar, hydrogen-bonding, or shear between the silicates and polymers. Although the enhancement of tensile properties in these nanostructured polymers from their pristine state was large, the amount of silicates added was quite substantial and is comparable to the amount of inorganics added in conventional composites. This leads us to the question of whether we can improve the tensile properties of polyurethane to the same extent not by resorting to the amount of modified silicates but by altering its morphology and molecular structure. In some studies, swelling agents were directly involved in the polymerization process and resulted in exfoliated structures of silicates in the polymer.<sup>8–14,22</sup> In the present study, we choose chemical compounds that contained one to three hydroxyl groups and one amine group for modifying montmorillonites, and these compounds are noted as reactive swelling agents. These reactive swelling agents have dual functions. The amine group in these reactive swelling agents was converted into an onium form to replace the metal ions in the gallery of the silicates for intercalation, and the available hydroxyl functional groups can react with the isocyanate groups of the polyurethane prepolymer.

\* To whom correspondence should be addressed. Tel: 886-35-731871. Fax: 886-35-724727. E-mail: khwei@cc.nctu.edu.tw.

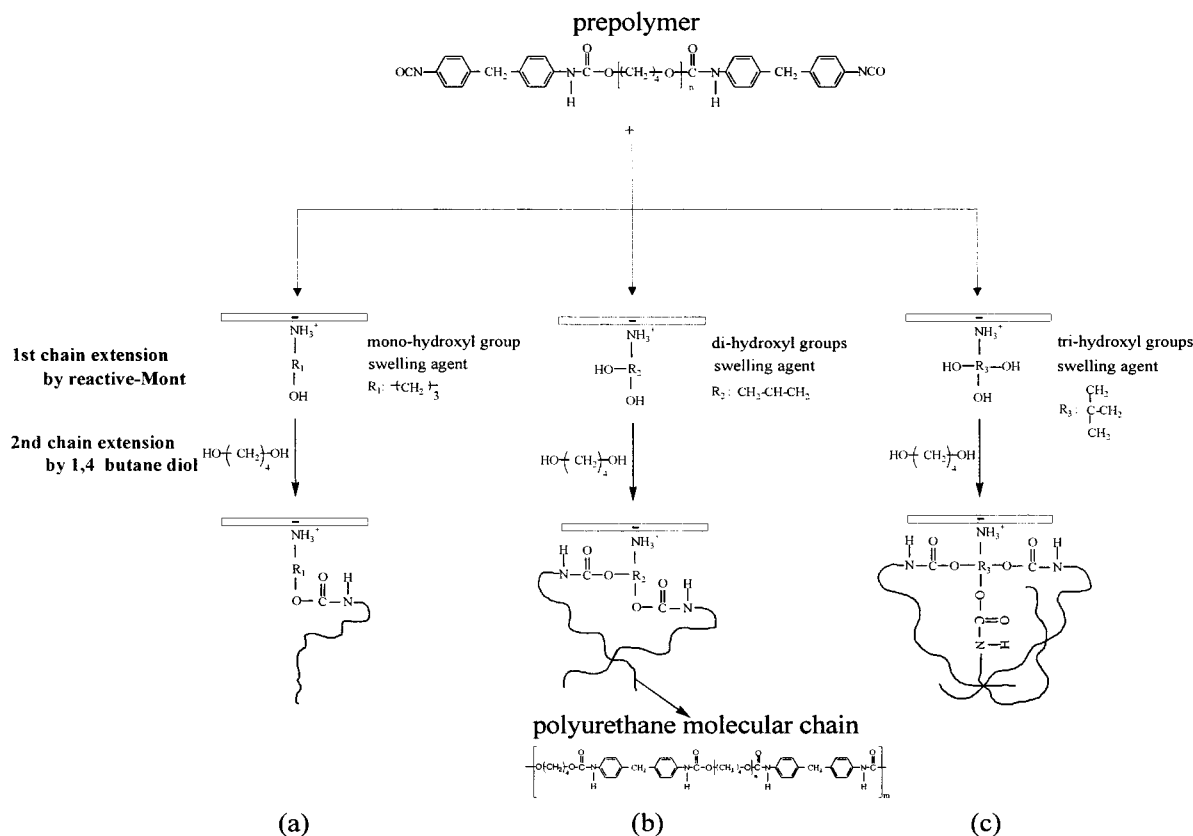


**Figure 1.** Schematic drawings of the molecular architecture of tethered layered silicates/polyurethane nanocomposites through reactive swelling agents containing (a) monohydroxyl groups, (b) dihydroxyl groups, or (c) trihydroxyl groups.

Montmorillonite modified by the reactive swelling agents was termed reactive-Mont. When the number of hydroxyl groups in the swelling agent was more than two, the reactive-Mont can be treated as a pseudo chain extender along with the regular chain extender (1,4-butanediol) for extending prepolymer chains, as shown in Figure 1. In Figure 1a, the monohydroxyl-group swelling-agent-modified silicate is only able to form a covalent bond and to hang on to the end of a polyurethane molecular chain. In Figure 1b, the dihydroxyl-group swelling-agent-modified silicate can form two covalent bonds with two polyurethane molecular chains, leading to a longer polymer chain length. In Figure 1c, the trihydroxyl-group swelling-agent-modified silicate becomes the connecting point of three polymer chains, leading to a branched structure. The montmorillonites in the nanostructured composites in the present study are defined as tethered-Mont as opposed to untethered-Mont, where modified montmorillonites are trapped in polyurethane by physical mixing, as carried out in previous studies. The intercalation force for attaining an exfoliated structure of silicates in polyurethane apparently reached the maximum in the case of a trihydroxyl-group swelling agent. With this new approach, we would like to investigate the degree of hydrogen bonding in the hard segments as well as the morphology and tensile mechanical properties of tethered layered silicates/polyurethane nanocomposites formed through the pseudo and regular chain extender.

## Experimental Section

**Materials.** Source clay Swy-2 (Wyoming  $\text{Na}^+$ -montmorillonite) was obtained from the Clay Minerals Depository at the University of Missouri, Columbia, MO. Swy-2  $\text{Na}^+$ -montmorillonite having a cationic exchange capacity of 76.4 mequiv/

100 g was screened with a sieve of 325 mesh to remove the larger montmorillonite agglomerates. As-received swelling agents including 3-amino-1-propanol (99%, Acros), 3-amino-1,2-propandiol (98%, Acros), tris(hydroxymethyl)aminomethane (99%, Merck), and dodecylamine (98%, Merck) were treated with hydrochloric acid, and they were termed 1OH, 2OH, 3OH, and 12CH<sub>3</sub>, respectively. The detailed process of modifying montmorillonite with swelling agents has been described elsewhere.<sup>20</sup> Montmorillonites modified with 1OH, 2OH, 3OH, and 12CH<sub>3</sub> were noted as 1OH-Mont, 2OH-Mont, 3OH-Mont, and 12CH<sub>3</sub>-Mont, respectively. The exchanged portion of sodium cations in the intergalleries of silicates was determined by the difference in weight between the montmorillonite and the swelling-agent-modified montmorillonite in the temperature range from 120 to 800 °C in the thermogravimetric analysis (TGA).<sup>10</sup> The exchanged portions of 1OH-Mont, 2OH-Mont, or 3OH-Mont and 12CH<sub>3</sub>-Mont were about 50% and 90%, respectively. Hence, the area density of the reactive swelling agent is about one per 400–676 Å<sup>2</sup> on the silicates. Poly(tetramethylene glycol) (PTMEG;  $M_n = 1000$ , Aldrich) was dehydrated under vacuum in an oven at 60 °C for 2 days. 4,4'-Diphenylmethane diisocyanate (MDI; Aldrich) was melted and pressure-filtered under N<sub>2</sub> at 60 °C, followed by recrystallization from hexane in an ice bath. Dimethylformamide (DMF; 99%, Fisher) and 1,4-butanediol (1,4-BD; Lancaster) were dried over calcium hydride for 2 days and were then vacuum-distilled. Polyurethane containing a 39 wt % hard segment (PU39) was produced by first reacting MDI and PTMEG at an equivalent weight ratio of 2:1 in 35 mL of a DMF solvent at 90 °C for 2 h to form the prepolymer. Then, 1,4-BD in 10 mL of DMF was added to the prepolymer solution and was stirred for 2 h to form a polyurethane solution. The solid content of these polymer solutions was 30 wt %. Subsequently, the solution was cast in a mold to heat at 70 °C for 24 h to complete the polymerization and remove solvent. For preparation of the tethered-Mont/polyurethane nanocomposites after synthesizing the polyurethane prepolymers, different amounts of reactive-Monts were added to the prepolymer solution,

**Table 1. Compositions and Characteristics of Polyurethane Nanocomposites at Different Compositions**

		contents of Mont (wt %)	MDI/PTMEG/1,4-BD/ swelling agents <sup>b</sup>	molecular weight <sup>d</sup>	$T_{g,soft}$ (°C) <sup>e</sup>	hydrogen-bonding index ( $R$ ) <sup>f</sup>
pure polyurethane	PU39	0	2/1/1/0	25 000	-53	0.931
	1OH/PU39 <sup>a</sup>	0	2/1/0.997/0.003 <sup>c</sup>	23 000	-54	0.933
	2OH/PU39 <sup>a</sup>	0	2/1/0.994/0.006 <sup>c</sup>	23 000	-53	0.930
	3OH/PU39 <sup>a</sup>	0	2/1/0.991/0.009 <sup>c</sup>	24 000	-54	0.931
untethered-Mont/ polyurethane <sup>a</sup>	12CH <sub>3</sub> -Mont in PU39	1	2/1/1/0	23 000	-52	0.928
		3	2/1/1/0	24 000	-54	0.925
		5	2/1/1/0	23 000	-53	0.925
tethered-Mont/ polyurethane	1OH-Mont in PU39	1	2/1/0.997/0.003	15 000	-52	0.926
		3	2/1/0.991/0.009	13 000	-52	0.924
		5	2/1/0.984/0.016	12 000	-53	0.924
	2OH-Mont in PU39	1	2/1/0.994/0.006	19 000	-54	0.915
		3	2/1/0.982/0.018	18 000	-52	0.901
		5	2/1/0.969/0.031	16 000	-53	0.885
	3OH-Mont in PU39	1	2/1/0.991/0.009	23 000	-53	0.863
		3	2/1/0.972/0.028	22 000	-52	0.847
		5	2/1/0.953/0.047	21 000	-53	0.821

<sup>a</sup> Control experiments. <sup>b</sup> Equivalent weight ratio (NCO/OH). <sup>c</sup> The corresponding amount of swelling agents in 1 wt % tethered-Mont in PU39. <sup>d</sup> Weight molecular weight of recovered polyurethane. <sup>e</sup> The glass transition temperature of the soft-segment phase of polyurethane obtained from DSC. <sup>f</sup> The hydrogen-bonding index obtained from the  $A_{1709}/A_{1733}$  in the FTIR curve.

followed by 1,4-BD. Two control experiments were performed. For the tethered-Mont/polyurethane case, the prepolymer was reacted with the same amount of reactive swelling agents as that used in the case of PU39 containing 1 wt % tethered-Monts along with 1,4-BD at 90 °C for 2 h. As to the untethered-Mont/polyurethane nanocomposites case, different amounts of 12CH<sub>3</sub>-Mont were added into the polyurethane solution and stirred at 90 °C for 4 h. The compositions of these samples are given in Table 1.

**Characterization.** Wide-angle X-ray diffraction (WAXD) experiments were performed by using a Mac Science M18 X-ray diffractometer. The X-ray beam was generated from nickel-filtered Cu K $\alpha$  ( $\lambda = 0.154$  nm) radiation in a sealed tube operated at 50 kV and 250 mA. The diffraction curves were obtained from 3° to 10° at a scan rate of 1°/min. The molecular weights of the recovered<sup>17</sup> polyurethanes and the pristine polyurethane were determined by a Waters 510 gel permeation chromatography (GPC) system with DMF as the solvent. The calibration curves for GPC were obtained by using polystyrene and poly(ethylene glycol) standards. Differential scanning calorimetry analyses over the temperature range from -100 to 220 °C were conducted on a Dupont DSC 2910 at a heating rate of 20 °C/min under a nitrogen purge. Fourier-transformed infrared spectroscopy (FTIR) experiments were performed with a Nicolet Omnic 3 spectrometer at a resolution of 4 cm<sup>-1</sup>. The samples for the FTIR study were prepared by first coating pristine polyurethane or nanocomposite solutions on KBr disks, and then removing the solvent in a vacuum oven at 70 °C for 24 h. Tensile strength tests were carried out on the samples with an Instron 4468 machine according to the specifications of ASTM D882. The sample sizes were 100 mm  $\times$  10 mm  $\times$  1 mm, and the crosshead speed was set at 500 mm/min. For each data point, five samples were tested, and the average value was taken. The samples for the transmission electron microscopy (TEM) study were prepared as described in a previous paper.<sup>27</sup>

## Results and Discussion

The WAXD curves of the ground montmorillonite (Mont), the reactive-Monts such as 1OH-Mont, 2OH-Mont, and 3OH-Mont, and the alkyl-Mont, 12CH<sub>3</sub>-Mont, are presented in Figure 2. In Figure 2, a broad diffraction peak appeared at  $2\theta = 7.4^\circ$  for the ground Mont case. The rather weak and broad diffraction peaks appearing in the X-ray diffraction curve of ground montmorillonite are attributed to the nonuniform  $d$  spacings between the silicates in montmorillonite. The  $d$  spacing between the rather isotropic layered silicates

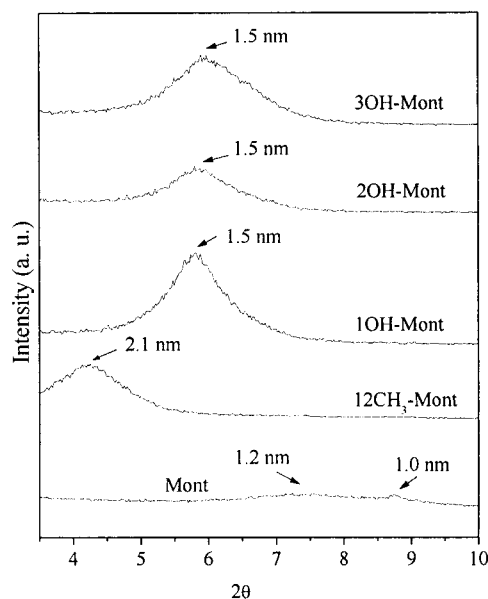


**Figure 2.** Wide-angle X-ray diffraction curves of reactive-Mont (1OH-Mont, 2OH-Mont, and 3OH-Mont), alkyl-Mont (12CH<sub>3</sub>-Mont), and montmorillonite (Mont).

in the Mont was about 1.2 nm. A strong diffraction peak at  $2\theta = 5.8^\circ$  was displayed in the WAXD of all reactive-Monts and is due to the diffraction of the (001) crystal surface of layered silicates. This implies that the inter-gallery distance has been intercalated to a distance of 1.5 nm. The resemblance in the  $d$  spacings of these reactive-Monts can be attributed to the fact that the molecular lengths of the three swelling agents (1OH, 2OH, and 3OH) are about the same. In the case of 12CH<sub>3</sub>-Mont, there was a diffraction peak at  $2\theta = 4.3^\circ$  in its WAXD curve, because of the longer molecular chain of 12CH<sub>3</sub> and corresponding to a  $d$  spacing of 2.1 nm in layered silicates.

The WAXD patterns of PU39 containing different amounts of 12CH<sub>3</sub>-Mont, 1OH-Mont, and 2OH-Mont are presented in parts a–c of Figure 3, respectively. In Figure 3a, three diffraction peaks at  $2\theta = 3.6^\circ$ ,  $3.7^\circ$ , and  $4.4^\circ$ , corresponding to  $d$  spacings of 2.5, 2.4, and 2.0 nm, are displayed for PU39 containing 1, 3, and 5 wt % 12CH<sub>3</sub>-Mont, respectively. This implies that an inter-

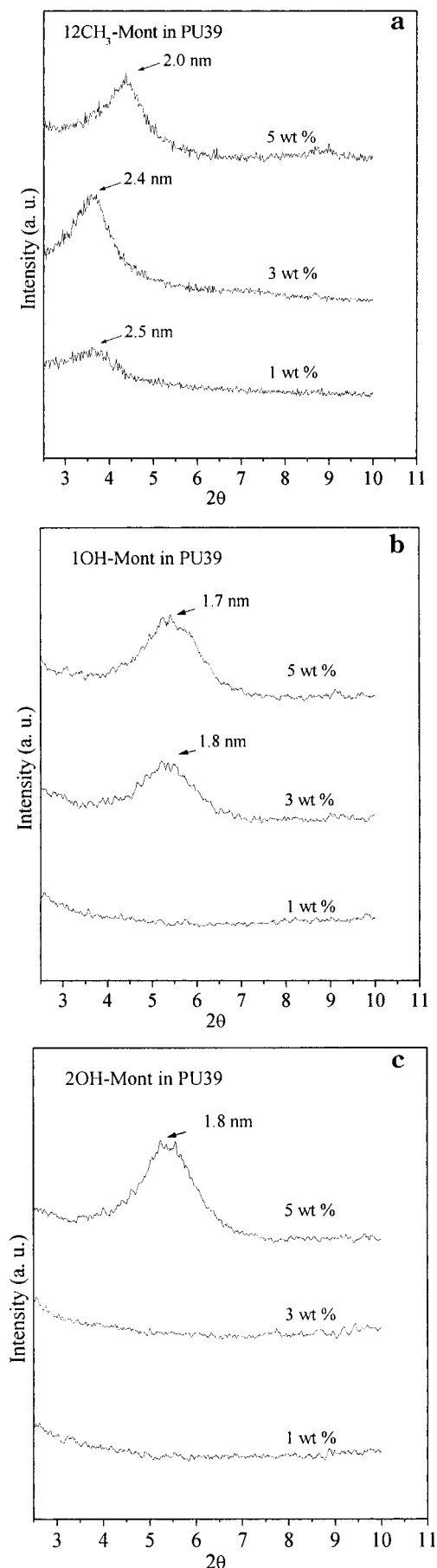


**Figure 3.** Wide-angle X-ray diffraction curves of PU39 containing 1, 3, and 5 wt % (a) 12CH<sub>3</sub>-Mont, (b) 1OH-Mont, and (c) 2OH-Mont.

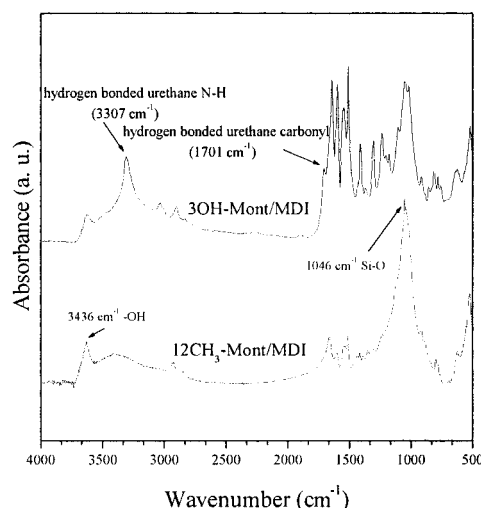


**Figure 4.** Fourier transform infrared spectra of 12CH<sub>3</sub>-Mont/MDI and 3OH-Mont/MDI.

calated nanostructure of silicate in the 12CH<sub>3</sub>-Mont/PU39 system (untethered case) has been formed, whereas in the tethered case shown in Figure 3b, one medium diffraction peak at  $2\theta = 5.0^\circ$  and another at  $2\theta = 5.2^\circ$ , corresponding to  $d$  spacings of 1.8 and 1.7 nm, appeared for PU39 containing 3 and 5 wt % 1OH-Mont, respectively. In Figure 3c, there is a medium diffraction peak at  $2\theta = 5.0^\circ$  with a  $d$  spacing of 1.8 nm for the case of 5 wt % 2OH-Mont in PU39. No WAXD peaks appeared between  $2\theta = 3^\circ$  and  $10^\circ$  for PU39 containing from 1 wt % up to 5 wt % 3OH-Mont. The WAXD peaks of the layered silicates appeared only when there are uniform  $d$  spacings between the silicates at certain orientations. There are no diffraction peaks between  $2\theta = 3^\circ$  and  $10^\circ$  for silicate/polyurethane nanocomposites, indicating that the  $d$  spacing between silicates is greater than 3 nm, but these silicates are not necessarily exfoliated. Two points can be deduced from the WAXD results of silicate/polyurethane nanocomposites. First, the extent of intercalation of the layered silicates in polyurethane increased with the reactivity (i.e., the number of functional groups) of modified silicates. Second, the dispersion of silicates in the tethered-Mont/PU case is different from that in the untethered-Mont/PU case.

To verify the differences in chemical structure between the polymer-trapping and the polymer-tethering cases, model compounds of untethered-Mont/PU and tethered-Mont/PU were prepared by mixing MDI with 12CH<sub>3</sub>-Mont (untethered case) and 3OH-Mont (tethered case) in DMF, respectively. The FTIR spectra of 12CH<sub>3</sub>-Mont/MDI and 3OH-Mont/MDI are shown in Figure 4. The hydrogen-bonded carbonyl and the hydrogen-bonded N-H bands from the urethane groups usually appeared at 1701 and 3307 cm<sup>-1</sup>, respectively, in the FTIR spectrum. There is no absorption peak at 1701 cm<sup>-1</sup> or at 3307 cm<sup>-1</sup> in the FTIR spectrum of 12CH<sub>3</sub>-Mont/MDI in Figure 4, indicating that there is no reaction between 12CH<sub>3</sub>-Mont and MDI. This implies that the polyurethane can just be absorbed on the silicate surface by the physical trap force in the untethered-Mont/PU system. In the case of the FTIR spectrum of 3OH-Mont/MDI, distinctive absorption bands at 1701 and 3307 cm<sup>-1</sup> are displayed. This is a direct result of urethane groups produced by a reaction of the hydroxyl groups in 3OH-Mont with the isocyanate groups of MDI. Hence, 3OH-Mont can be tethered to the polyurethane

chain through the formation of urethane bonds as confirmed in this FTIR study.

The most direct measure of the dispersion of these nanometer-scale silicates in polyurethane can typically be found in the TEM micrographs of the cross section of polymer nanocomposites as demonstrated in most of the literature.<sup>9,10,13,14,22,24</sup> In Figure 5a, in the case of PU39 containing 1 wt % 1OH-Mont, intercalated domains (marked as I) having a collection of four to five nearly parallel layered silicates with basal spacings from 3 to 6 nm were observed. The thickness of the layered silicate (dark lines) was about 1.0 nm. For the case of PU39 containing 1 wt % 2OH-Mont, the space between layered silicates was enlarged to between 4 and 7 nm, and a small portion of silicates was exfoliated (marked as II), as shown in Figure 5b. In Figure 5c, for PU39 containing 1 wt % 3OH-Mont, the space between layered silicates was about 4–10 nm, and a larger portion of silicates became exfoliated as compared to PU39 containing 1 wt % 2OH-Mont. The dispersion of the silicates in polyurethane can actually adopt a bimodal structure, which consists of both intercalated and exfoliated states, as shown in Figure 5c. Therefore, it is quite clear that, as the number of functional groups in the modified silicates increases, the dispersion of silicates in polyurethane changed from an intercalated to an exfoliated structure. This transformation in the morphology of the polyurethane nanocomposites is most likely due to an increase of the intercalation force between silicates as a result of the multiple-polyurethane-chains grafting on silicates (tethered-Mont).

From a polymer science point of view, the molecular weight of polyurethane in these nanocomposites must be examined. The molecular weights of the pristine, the control, and the recovered<sup>17</sup> polyurethanes are given in Table 1. In Table 1, the molecular weights of 1OH/PU39, 2OH/PU39, and 3OH/PU39 were slightly lower as compared to that of pristine polyurethane, with the highest molecular weight for 3OH/PU39. This implies that the reactivity of 3OH toward the isocyanate group of the prepolymer is higher than that of 1OH and 2OH. In the case of 12CH<sub>3</sub>-Mont/PU39, the molecular weight of the recovered polyurethane was close to that of pristine PU39, indicating that the mixing of the alkyl silicate with polyurethane was purely physical. On the other hand, the molecular weight of the recovered polyurethane from the tethered-Mont/PU was much lower than that of the pristine PU39. The extent of the reduction in molecular weight of recovered polyurethane depends on two counteracting factors: the hindrance effect on the chain-extending reaction of a polyurethane prepolymer during synthesis by the relatively large silicates and the reactivity of the swelling agents. In the control experiments, about 0.3 wt % of 1OH, 2OH, and 3OH along with 1,4-BD were added to the polyurethane prepolymer, and the molecular weights of 1OH/PU39, 2OH/PU39, and 3OH/PU39 are about the same as that of pristine PU39. In the synthesis of tethered-Mont/PU, the reactive-Mont, which was treated as a pseudo chain extender, was added to the polyurethane prepolymer followed by the addition of another chain extender (1,4-BD). In this synthesis sequence, the reactivity of tethered-Mont is critical in determining the final molecular weight of polyurethane in the nanocomposites. Table 1 shows that the molecular weight of polyurethane in PU39 containing 1 wt % 1OH-Mont and 2OH-Mont reduced dramatically but not in the case of

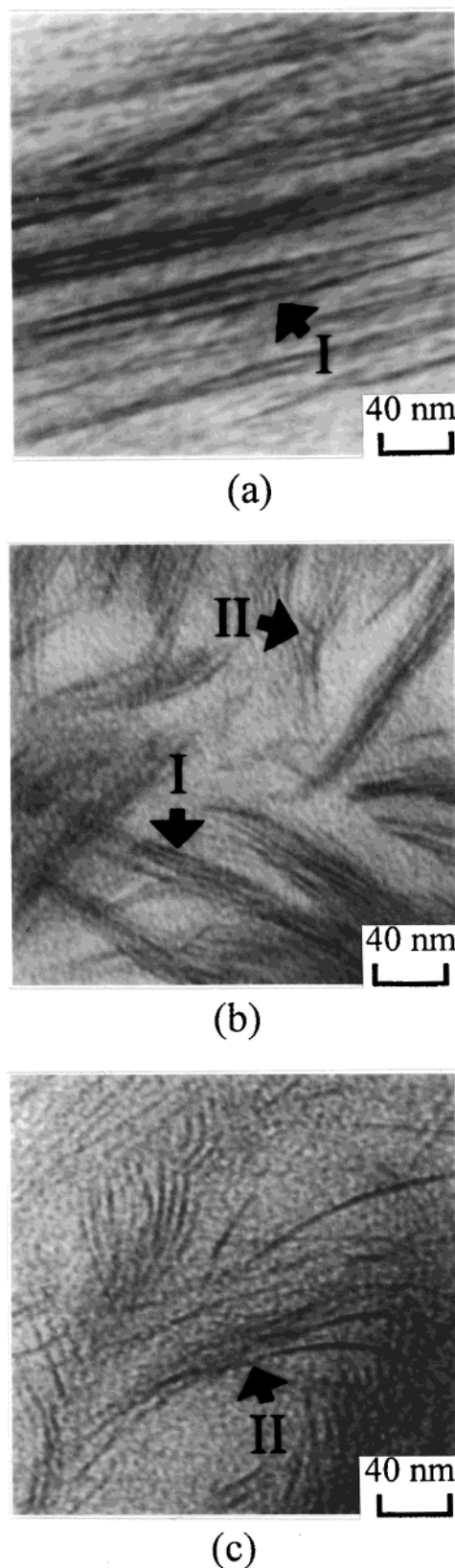


**Figure 5.** Transmission electron microscopy micrographs of the cross-sectional views of PU39 containing (a) 1 wt % 1OH-Mont (b) 1 wt % 2OH-Mont, and (c) 1 wt % 3OH-Mont: (I) indicated intercalated structure; (II) indicated exfoliated structure.

PU39 containing 1 wt % 3OH-Mont, as compared to that of pristine PU39. This phenomenon can best be explained by the molecular architectures of swelling-agent-modified silicates, as demonstrated in Figure 1a–

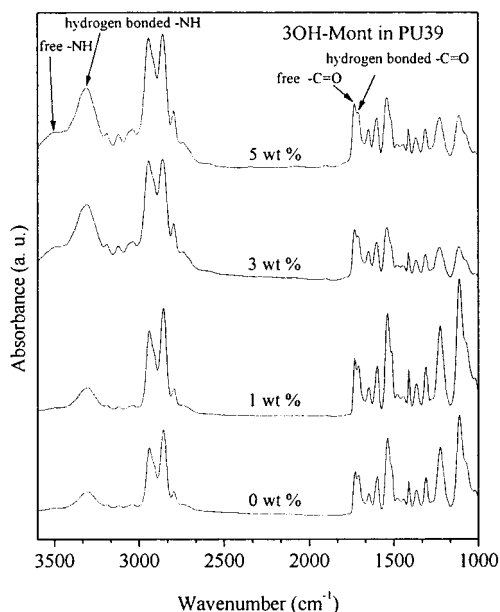


**Figure 6.** Fourier transform infrared spectra of PU39 containing 0, 1, 3, and 5 wt % 3OH-Mont.

c, where the hydroxyl groups in 1OH-Mont or 2OH-Mont might be prevented from reacting with isocyanate groups in the polyurethane prepolymer because of the steric effect of the neighboring swelling agents. However, in the case of 3OH-Mont, one hydroxyl group is sticking out from the surface of the silicate and can react with isocyanate of the polyurethane prepolymer even if the two  $-OH$  groups were blocked by neighboring swelling agents. Consequently, the molecular weight of polyurethane in PU39 containing 3OH-Mont is reasonably close to that of pristine PU39. The reduction in molecular weight of polyurethane in tethered-Mont/PU nanocomposites becomes more pronounced as the amount of reactive-Mont increases, because the reactive-Mont is a much less reactive pseudo chain extender.

The thermal analysis results and the hydrogen-bonding index of polyurethane nanocomposites measured by DSC and FTIR are also given in Table 1. In Table 1, the glass transition temperature of the soft-segment phase ( $T_{g,soft}$ ) of PU39 was  $-53\text{ }^{\circ}\text{C}$ , and the glass transition of the hard-segment phase was not detectable in the DSC measurements because of low hard-segment content and small heat capacity differences at the hard segment's glass transition ( $\Delta C_{p(hard)} = 0.38\text{ J/g }^{\circ}\text{C}$ ).<sup>31</sup> There were essentially no changes in the glass transition temperatures of the soft-segment phase in PU39 nanocomposites because DSC cannot probe the glass transition temperature of polymer chains close to the silicates. Thus, the measured glass transition temperature is that of the soft-segment phase far away from the silicates and is the same as that for bulk polyurethane.

The FTIR spectra of PU39 containing different amounts of 3OH-Mont are shown in Figure 6. In Figure 6, only related bands are labeled, and the detailed description of other bands in polyurethane can be found elsewhere.<sup>2,3</sup> The fact that the distinctive bands of PU39 nanocomposites were the same as those of the pristine PU39 indicates that there are no new chemical bonds formed in the nanocomposites. The degree of the hard-segment hydrogen bonding in polyurethane, defined as the carbonyl hydrogen-bonding indices ( $R$ ), can be

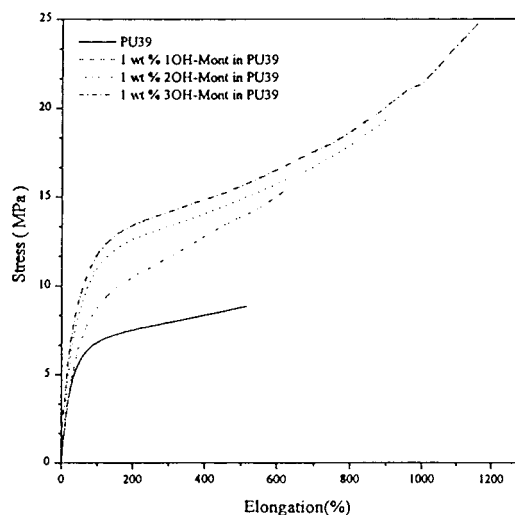


**Figure 7.** Stress-strain curves of PU39 containing 1 wt % tethered-Mont.

obtained from the ratio of the hydrogen-bonding carbonyl peak at  $1709\text{ cm}^{-1}$  to the free carbonyl peak at  $1733\text{ cm}^{-1}$ . The calculation of  $R$  is based upon the formula described in previous papers,<sup>2,3,28</sup> and the results are given in Table 1. In Table 1, the  $R$  values of PU39 nanocomposites are always smaller than that for pristine PU39, resulting from the fact that the relatively large silicates hinder the hydrogen bonding between hard segments. The  $R$  values decrease with increasing amount of silicate and level off at 5 wt % tethered-Mont content. Moreover, the extent of reduction in the  $R$  value increases with the number of functional groups in the swelling agent, and the smallest  $R$  value occurs in the case of PU39 containing 5 wt % 3OH-Mont, which was 12% smaller than that of pristine PU39. This is attributed to a more exfoliated dispersion of silicate in polyurethane caused by the higher reactivity of the swelling agent, which in turn creates a larger interfacial area between silicates and polyurethane. Hence, the hard-segment hydrogen bonding in the hard-segment phase of PU39 is more greatly retarded in the presence of 3OH-Mont than in the presence of 12CH<sub>3</sub>-Mont.

For the tensile properties of these polyurethane nanocomposites, typical stress-strain curves of PU39 containing 1 wt % tethered-Mont are shown in Figure 7, where both the modulus and the elongation to break of PU39 nanocomposites increase substantially. The more detailed tensile mechanical properties of PU39 nanocomposites at different compositions are given in Table 2. In Table 2, the increases in the mechanical properties of PU39 nanocomposites as compared to that of pristine polyurethane were attributed mainly to the layered silicates tethered to the PU39 molecule through the reactive swelling agent rather than the reactive swelling agents themselves. This argument can be supported by the results of the control experiment, which showed that a rather small increase in the mechanical properties of 3OH/PU39 occurred as compared to that of the pristine polyurethane. To isolate the effect of polymer tethering, the other compositions in polyurethane nanocomposites were kept the same. We choose 1 wt % 12CH<sub>3</sub>-Mont in PU39 (untethered case) and 1 wt % 3OH-Mont in PU39 (tethered case) for comparison because the molecular weight of polyurethane in the two cases is about the same as that of the pristine PU39, as given in Table 1. In Table 2, for

**Table 2. Mechanical Properties of Polyurethane Nanocomposites at Different Compositions**

		loading in PU39 (wt %)	Young's modulus (MPa)	tensile strength (MPa)	elongation to break (%)	increase (%) of mechanical properties at 1 wt % silicate content <sup>c</sup>		
						Young's modulus	tensile strength	elongation
pure polyurethane	pure PU39	0	20.97 ± 0.39	8.9 ± 0.3	516 ± 23			
	1OH <sup>a</sup> in PU39	0.028 <sup>b</sup>	20.78 ± 0.25	8.7 ± 0.6	510 ± 40			
	2OH <sup>a</sup> in PU39	0.034 <sup>b</sup>	21.27 ± 0.20	9.0 ± 0.4	520 ± 26			
	3OH <sup>a</sup> in PU39	0.045 <sup>b</sup>	21.56 ± 0.28	9.3 ± 0.6	530 ± 33			
untethered-Mont/ polyurethane <sup>a</sup>	12CH <sub>3</sub> -Mont in PU39	1	21.25 ± 0.22	9.0 ± 0.9	522 ± 22	+1	+1	+1
		3	21.85 ± 0.31	9.6 ± 0.7	525 ± 31			
		5	22.48 ± 0.12	10.8 ± 0.3	536 ± 35			
tethered-Mont/ polyurethane	1OH-Mont in PU39	1	24.70 ± 0.36	17.1 ± 0.8	673 ± 27	+18	+92	+30
		3	23.03 ± 0.28	15.0 ± 0.6	638 ± 20			
		5	21.07 ± 0.36	12.8 ± 0.5	603 ± 15			
	2OH-Mont in PU39	1	26.75 ± 0.50	19.5 ± 1.1	909 ± 14	+28	+119	+76
		3	23.52 ± 0.47	17.9 ± 0.8	872 ± 24			
		5	22.25 ± 0.70	16.6 ± 0.5	883 ± 13			
	3OH-Mont in PU39	1	28.03 ± 0.30	23.6 ± 0.4	1167 ± 35	+34	+165	+126
		3	25.87 ± 0.33	21.5 ± 0.6	1092 ± 39			
		5	24.99 ± 0.38	20.0 ± 1.4	1076 ± 28			

<sup>a</sup> Control experiments. <sup>b</sup> The corresponding amounts of swelling agents in 1 wt % tethered-Mont in PU39. <sup>c</sup> The increases of Young's modulus, tensile strength, and elongation of polyurethane nanocomposites at 1 wt % silicate content as compared with those of pristine polyurethane were chosen because the molecular weights of polyurethane are about the same in these cases.

the untethered-Mont/PU case, the Young's modulus, tensile strength, and elongation of PU39 containing 1 wt % 12CH<sub>3</sub>-Mont are all about 1% higher than those of pristine PU39, whereas in the case of tethered-Mont/PU, the Young's modulus, tensile strength, and elongation of PU39 having 1 wt % 3OH-Mont are 34%, 165%, and 126% higher than those of pristine PU39, respectively. Therefore, the efficiency of the enhancement in the tensile properties of polyurethane due to the tethered-Mont is dramatically larger than that in the untethered-Mont case.

Additionally, in Table 2, the Young's modulus of PU39 containing 1 wt % 1OH-Mont, 2OH-Mont, and 3OH-Mont were 18%, 28%, and 34% higher than that of the pristine PU39, respectively. The largest increase in Young's modulus occurred in the case of 1 wt % 3OH-Mont in PU39, because of its exfoliated layered-silicates structure. The modulus of these PU nanocomposites reaches a maximum value when the amount of tethered-Mont is 1 wt %. This type of behavior can be explained by two adverse effects and one advantageous effect induced by the inclusion of tethered-Monts in polyurethane. As described in previous sections of this paper, both the molecular weight and the hydrogen bonding in the hard-segment phase of polyurethane in the nanocomposites decreased as the amount of tethered-Mont increased, resulting in a substantial reduction in the modulus of the tethered-Mont/PU. These two effects offset the presumed enhancement in the modulus of the nanocomposites by the stiff, layered silicates. The combined effects produced a maximum value for the modulus of the PU39 nanocomposites at 1 wt % tethered-Monts content. The increase in the tensile strength depends on the strength of the interfacial bonding between Mont and PU39 molecules. Because 3OH-Mont provided more linking points with polyurethane molecules than 1OH-Mont and 2OH-Mont, the bonding in 3OH-Mont/PU39 is the strongest, and this pseudo-branched structure resulted in a 1.7-fold increase in the tensile strength as compared to that of the pristine PU39. By the same reasoning, the elongation behavior of the tethered-Mont/PU is also determined by the

interfacial strength between polyurethane and silicates. The elongation to break of tethered-Mont/PU increased substantially as compared to that of pure PU39, with the largest increase (1.3-fold) recorded for PU39 containing 1 wt % 3OH-Mont. This phenomenon is quite possibly a result of the reinforced branched structure by tethered-Mont in polyurethane.

## Conclusions

High tensile strength and high elongation tethered silicates/polyurethane nanocomposites were synthesized by using multiple-functional-groups swelling-agent-modified silicates as pseudo chain extenders for polyurethane prepolymer. This approach resulted in a dramatic improvement in the tensile mechanical properties of the polyurethane nanocomposites as compared to their pristine state because of the tethering structure of silicates in polyurethane. Furthermore, the efficiency of the enhancement in the tensile properties of polyurethane due to the polymer tethering of silicates is much larger than that attributed to physical trapping of silicates in previous studies.

**Acknowledgment.** We appreciate the financial support provided by the National Science Council through Project NSC89-2218-E009-025 and the suggestions and comments of anonymous reviewers.

## References and Notes

- (1) Garrett, J. T.; Runt, J.; Lin, J. S. *Macromolecules* **2000**, *33*, 6353–6359.
- (2) Miller, J. A.; Lin, S. B.; Hwang, K. S.; Wu, K. S.; Gibson, P. E.; Cooper, S. L. *Macromolecules* **1985**, *18*, 32–44.
- (3) Wang, C. B.; Cooper, S. L. *Macromolecules* **1983**, *16*, 775–786.
- (4) Ziolo, R. F.; Giannelis, E. P.; Weinstein, B. A.; O'Horo, M. P.; Granguly, B. N.; Mehrota, V.; Russell, M. W.; Huffman, D. R. *Science* **1992**, *257*, 219–222.
- (5) Gleiter, H. *Adv. Mater.* **1992**, *4*, 474–481.
- (6) Komarneni, S. *J. Mater. Chem.* **1992**, *2*, 1219–1230.
- (7) Novak, B. M. *Adv. Mater.* **1993**, *5*, 422–433.
- (8) Usuki, A.; Kawasumi, M.; Kojima, Y.; Okada, A.; Kurauchi, T.; Kamigaito, O. *J. Mater. Res.* **1993**, *8*, 1174–1178.

- (9) Usuki, A.; Kawasumi, M.; Kojima, Y.; Okada, A.; Fukushima, Y.; Kurauchi, T.; Kamigaito, O. *J. Mater. Res.* **1993**, *8*, 1179–1184.
- (10) Kojima, Y.; Usuki, A.; Kawasumi, M.; Okada, A.; Kurauchi, T.; Kamigaito, O. *J. Polym. Sci., Part A: Polym. Chem.* **1993**, *31*, 983–986.
- (11) Wang, M. S.; Pinnavaia, T. J. *Chem. Mater.* **1994**, *6*, 468–474.
- (12) Wang, Z.; Pinnavaia, T. J. *Chem. Mater.* **1998**, *10*, 1820–1826.
- (13) Zeng, C.; Lee, L. J. *Macromolecules* **2001**, *34*, 4098–4103.
- (14) Weimer, M. W.; Chen, H.; Giannelis, E. P.; Sogah, D. Y. *J. Am. Chem. Soc.* **1999**, *121*, 1615–1616.
- (15) Bujdák, J.; Hackett, E.; Giannelis, E. P. *Chem. Mater.* **2000**, *12*, 2168–2174.
- (16) Hackett, E.; Manias, E.; Giannelis, E. P. *Chem. Mater.* **2000**, *12*, 2161–2167.
- (17) Messersmith, P. B.; Giannelis, E. P. *J. Polym. Sci., Part A: Polym. Chem.* **1995**, *33*, 1047–1057.
- (18) Lan, T.; Kaviratna, P. D.; Pinnavaia, T. J. *Chem. Mater.* **1994**, *6*, 573–575.
- (19) Tyan, H. L.; Liu, Y. C.; Wei, K. H. *Polymer* **1999**, *40*, 4877–4886.
- (20) Tyan, H. L.; Liu, Y. C.; Wei, K. H. *Chem. Mater.* **1999**, *11*, 1942–1947.
- (21) Tyan, H. L.; Wei, K. H.; Hsieh, T. E. *J. Polym. Sci., Part B: Polym. Phys.* **2000**, *38*, 2873–2878.
- (22) Tyan, H. L.; Leu, C. M.; Wei, K. H. *Chem. Mater.* **2001**, *13*, 222–226.
- (23) Wang, Z.; Pinnavaia, T. J. *Chem. Mater.* **1998**, *10*, 3769–3771.
- (24) Zilg, C.; Thomann, R.; Mulhaupt, R.; Finter, J. *Adv. Mater.* **1999**, *11*, 49–52.
- (25) Xu, R.; Manias, E.; Snyder, A. J.; Runt, J. *Macromolecules* **2001**, *34*, 337–339.
- (26) Chen, T. K.; Tien, Y. I.; Wei, K. H. *J. Polym. Sci., Part A: Polym. Chem.* **1999**, *37*, 2225–2233.
- (27) Chen, T. K.; Tien, Y. I.; Wei, K. H. *Polymer* **2000**, *41*, 1345–1353.
- (28) Tien, Y. I.; Wei, K. H. *Polymer* **2001**, *42*, 3213–3221.
- (29) Tien, Y. I.; Wei, K. H. *J. Polym. Res.* **2000**, *7*, 245–250.
- (30) Pinnavaia, T. J. *Science* **1983**, *220*, 365–371.
- (31) Chen, T. K.; Chui, J. Y.; Shieh, T. S. *Macromolecules* **1997**, *30*, 5068–5074.

MA010551P